

NUMERICAL MODEL OF PLASMA CONFINEMENT

J. C. Sprott and E. J. Strait

January 1975

(This paper submitted to IEEE - Transactions on Plasma Science)

PLP 607

Plasma Studies
University of Wisconsin

These PLP Reports are informal and preliminary and as such may contain errors not yet eliminated. They are for private circulation only and are not to be further transmitted without consent of the authors and major professor.

Numerical Model of Plasma Confinement

J. C. Sprott and E. J. Strait
Department of Physics
University of Wisconsin
Madison, Wisconsin 53706

I. INTRODUCTION

This paper describes SIMULT¹, a fast, simple, time-dependent, zero-dimensional computer model for plasmas confined in cylindrical or large aspect ratio toroidal devices, and compares its predictions with experimental data. This paper deals in particular with a version that models hydrogen ECRH microwave plasmas in the Wisconsin Levitated Toroidal Octupole², but the extension to other devices and heating methods is straightforward.

The development of this program was motivated by a desire to understand the energy and particle loss mechanisms in toroidal devices, and therefore only those mechanisms have been included which can be justified from theory or independent experimental measurements (e.g., collision cross sections). No adjustable parameters were allowed for fitting predictions to experimental measurements. The hope was that discrepancies would appear, and terms could then be added and adjusted to account for the discrepancies, thereby giving information about any anomalous heating or loss mechanisms.

All terms are spatially averaged in some appropriate way, and the electron and ion velocity distributions are assumed to be Maxwellian, so the major quantities which are predicted are the spatially averaged values of charged particle density, electron temperature, and ion temperature. Differential equations for the rate of change of each of these quantities are solved by a second order iterative method to predict their values at successive time intervals. These equations depend only on average quantities, all spatial and velocity distributions having been removed by averaging.

II. DEFINITION OF SYMBOLS

The symbols used below in the description of the various terms, and their units, are:

n = average electron (ion) density ($10^9/\text{cm}^3$)

n_0 = average neutral molecule density ($10^9/\text{cm}^3$)

n_{oi} = initial neutral molecule density ($10^9/\text{cm}^3$)

P_{oi} = initial neutral pressure (10^{-5} torr)

U_e = average electron energy density (10^9 eV/ cm^3)

U_i = average ion energy density (10^9 eV/ cm^3)

T_e = average electron temperature (eV)

T_i = average ion temperature (eV)

T_w = plasma chamber wall temperature (eV)

B = average magnetic field strength (kG)

B_0 = peak magnetic field strength (kG)

\dot{B} = dB/dt (kG/sec)

a = minor radius of plasma (cm)

L = length of plasma (or major circumference) (cm)

A_0 = obstacle area (cm^2)

P = microwave power (watts)

f = microwave frequency (GHz)

Q_0 = unperturbed cavity Q of plasma chamber

S = pumping speed of vacuum system (liters/sec)

$t = \text{time (sec)}$

For the levitated toroidal octupole, we take the values:

$$T_w = .025 \text{ eV}$$

$$a = 50 \text{ cm}$$

$$L = 800 \text{ cm}$$

$$Q_o = 20 \times 10^4$$

$$S = 10^3 \text{ liters/sec}$$

III. TERMS USED IN COMPUTATION

A. Magnetic Field

Any time-dependent magnetic field can be specified. The levitated octupole is usually operated with a half-sine-wave pulse of the form:

$$B_{\text{vac}} = B_0 e^{-t/\tau} \sin \omega t$$

where $\tau = .086$ sec and $\omega = (\pi/.043)$ sec⁻¹. The magnetic field is then corrected for finite beta:

$$B = [B_{\text{vac}}^2 - 4.05 \times 10^{-8} n(T_e + T_i)]^{1/2}$$

B. Neutral Density

The neutral hydrogen gas is assumed to consist of thermal ($T = T_w$) molecules. The initial value of neutral density is an experimental parameter which must be set. At each time step the density is calculated according to

$$\frac{dn_o}{dt} = \left[-g \left(\frac{dn}{dt} \Big|_{\text{diffusion}} + \frac{dn}{dt} \Big|_{\text{obstacles}} + \frac{dn}{dt} \Big|_{\text{field decay}} \right) - \frac{dn}{dt} \Big|_{\text{ionization}} - 318.0 \text{ } \$ (n_o - n_{oi})/a^2 L \right] \exp \left(- \frac{4.1 \times 10^{-7}}{T_w} \frac{a}{n_o} \frac{dn}{dt} \Big|_{\text{ionization}} \right)$$

The exponential factor accounts for the finite penetration depth of neutrals into the plasma. g represents the number of reflux neutrals

created by each lost electron-ion pair striking a wall or obstacle. It is taken from preliminary experimental measurements³ to be $g = 1 + .002 T_e$. If the neutral density is increasing in time due to wall reflux then the derivative is limited by

$$\frac{dn_o}{dt} \leq 1.9 \times 10^5 \frac{n_o}{a}$$

representing the transit time of a neutral from the edge to the center of the plasma.

Some attempt was also made to include a component of fast Franck-Condon neutrals. The treatment was very crude, but for all experiments simulated so far the Franck-Condon neutrals were quite unimportant.

C. Plasma Density

For microwave plasmas the initial value of plasma density is usually taken to be $10^6/\text{cm}^3$, but this can be varied by two orders of magnitude or more without significant effect on the results.

$\frac{dn}{dt}$ is the sum of the following four terms:

1. Ionization

The rate for electron-neutral collisional ionization for a Maxwellian electron distribution in a cold hydrogen gas is given by⁴

$$\left. \frac{dn}{dt} \right|_{\text{ionization}} = \frac{371.0 e^{-R}}{(1+R) T_e} \left(\frac{1}{20+R} + en(1.25(1 + 1/R)) \right)$$

where $R = 15.6/T_e$.

2. Diffusion

Classical diffusion due to electron-ion and electron-neutral collisions is given by⁵

$$\left. \frac{dn}{dt} \right|_{\text{diffusion}} = - .33 \frac{n^2}{B^2 a^2 T_e^{1/2}} - 10^{-3} \frac{n n_0 T_e}{B^2 a^2}$$

The ambipolar electric field has been considered, but ion-neutral collisions have been neglected since they amount to only a 1.2% correction to the diffusion rate.

3. Obstacles

Hoop supports and probes which intercept the plasma are assumed to collect particles at the rate given by the ion saturation current to a Langmuir probe in an isotropic plasma:

$$\left. \frac{dn}{dt} \right|_{\text{obstacles}} = - 2 \times 10^5 \frac{n A_0 \sqrt{T_e + T_i}}{a_L^2}$$

where A_0 is the area presented to the plasma by such obstacles.

For the levitated octupole operating in the supported mode, $A_0 = 700 \text{ cm}^2$ for the hoop supports. In the levitated mode A_0 corresponds only to the area of any probes in the plasma.

4. Field Decay

When \dot{B} is negative, field lines leaving the machine are assumed to carry plasma out with them at a rate given by

$$\left. \frac{dn}{dt} \right|_{\text{field decay}} = C \frac{\dot{B}}{B} n$$

where C is a constant of order unity which depends on the magnetic field configuration. $C \approx .5$ for an octupole.

D. Electron Energy Density

The initial value for T_e is usually taken as room temperature, but the results are insensitive to this. $\frac{dU_e}{dt}$ is calculated as the sum of the following six terms. Then

$$\frac{dT_e}{dt} = \left(\frac{3}{2} \frac{dU_e}{dt} - T_e \frac{dn}{dt} \right) / n.$$

1. Microwave Heating

The microwave heating rate is given by

$$\left. \frac{dU_e}{dt} \right|_{\text{microwaves}} = \frac{2 \times 10^9 P}{(1 + n_c/n) a^2 L}$$

where n_c is the density above which microwaves are totally absorbed. n_c is given very roughly by $n_c \approx 487 f^2/Q$ and for a toroidal octupole is given more precisely by⁶

$$n_c = \frac{f^2}{Q} [0.0045 (f/B)^4 + 123.0 (B/f)^{2/3}]$$

2. Ion Collisions

Classical electron-ion collisions result in an energy loss (ref. 7, p. 135)

$$\left. \frac{dU_e}{dt} \right|_{\text{ion collisions}} = - \frac{2.3 n_i^2 (T_e - T_i)}{T_e^{3/2}} \ln \left[\frac{5.2 \times 10^{11} T_e^3}{(40 + T_e)n} \right]$$

3. Excitation

An empirical fit to data⁴ gives losses by excitation of neutral molecules as

$$\left. \frac{dU_e}{dt} \right|_{\text{excitation}} = - 29.1 \exp \left(\frac{6.98}{T_e} \right) \left. \frac{dn}{dt} \right|_{\text{ionization}}$$

4. Bremsstrahlung

Electron-ion bremsstrahlung losses are given by (ref. 8, p. 233)

$$\left. \frac{dU_e}{dt} \right|_{\text{bremsstrahlung}} = - 10^{-4} n^2 T_e^{1/2}$$

5. Synchrotron Radiation

Electron synchrotron radiation, neglecting reabsorption and

wall reflection, is given by (ref. 8, p. 251).

$$\left. \frac{dU_e}{dt} \right|_{\text{synchrotron}} = - 3.87 \times 10^{-3} n B^2 T_e (1 + T_e / 2.04 \times 10^5)$$

6. Thermal Conduction

Heat conduction by particles lost due to classical diffusion², obstacles⁹, and field decay, is given by

$$\left. \frac{dU_e}{dt} \right|_{\text{thermal conduction}} = \left[2.5 \left. \frac{dn}{dt} \right|_{\text{diff.}} + 2.0 \left. \frac{dn}{dt} \right|_{\text{obst.}} + 1.5 \left. \frac{dn}{dt} \right|_{\text{f.d.}} \right] (T_e - T_w)$$

The factors larger than 3/2 for diffusion and obstacle losses account for the preferential loss of high energy particles.

E. Ion Energy Density

The initial value of T_i is usually taken as room temperature, but the results are insensitive to this. $\left. \frac{dU_e}{dt} \right|$ is calculated as the sum of the following four terms. Then $\frac{dT_i}{dt} = \left(\frac{3}{2} \left. \frac{dU_e}{dt} - T_i \left. \frac{dn}{dt} \right) \right) / n$.

1. Electron Collisions

Ions are heated by classical collisions with electrons:

$$\left. \frac{dU_i}{dt} \right|_{\text{electron collisions}} = - \left. \frac{dU_e}{dt} \right|_{\text{ion collisions}}$$

2. Charge Exchange

An approximate analytic form for charge-exchange losses, obtained by averaging cross sections found in the literature¹⁰, is

$$\left. \frac{dU_i}{dt} \right|_{\text{charge exchange}} = - .0732 n n_o T_i^{3/2} (1 + .00585 T_i^{3/2}) e^{-.0582 \sqrt{T_i}}$$

3. Thermal Conduction

This term is exactly analogous to that for electrons:

$$\left. \frac{dU_i}{dt} \right|_{\text{thermal conduction}} = \left[2.5 \left. \frac{dn}{dt} \right|_{\text{diff.}} + 2.0 \left. \frac{dn}{dt} \right|_{\text{obst.}} + 1.5 \left. \frac{dn}{dt} \right|_{\text{f.d.}} \right] (T_i - T_w)$$

4. Neutral Collisions

Energy lost due to elastic ion-neutral collisions, neglecting heating of the neutrals, is given in an approximate analytic form from cross sections found in the literature¹¹ by

$$\left. \frac{dU_i}{dt} \right|_{\text{neutral collisions}} = - 26.7 n n_o (T_i - T_w)^{1.05} (570 + T_i^{2.4})^{-.29}$$

IV. COMPARISON WITH EXPERIMENT

A. Description of Experiment

The Wisconsin Levitated Octupole¹ is a toroidal device of 139 cm major radius, and having a roughly square minor cross section with an average half-width, or "minor radius", of 58 cm. The magnetic field is provided by inductively-driven currents in four internal rings. The magnetic field is pulsed, having in normal operation the temporal shape of a damped half-sine-wave of 43 msec duration. The internal rings can be "levitated" by removing their supports, which otherwise extend through the plasma region, for about 20 msec.

Fig. (1) shows the theoretical magnetic field configuration.

This experiment used electron cyclotron resonant heating to produce the plasma. An amount of hydrogen gas, measured with a fast ion gauge, was puffed into the toroid and a 2.45 GHz, CW microwave source was switched on just before the magnetic field pulse. The microwaves were then switched off at 22 msec after the beginning of the field pulse. The amount of neutral gas admitted and the microwave power were both varied. At the peak of the pulse the maximum field strength at the inner wall was 5kG, giving an average field strength in the plasma region of about 1.6kG.

Fig. (2) shows the values predicted by SIMULT for n , T_e , and T_i as functions of time, for a typical set of experimental parameters.

T_e shows a large spike (several hundred eV) near the beginning of the pulse, as the entire microwave input power is absorbed by the small number of electrons present before the plasma density builds up. A burst of x-rays has been observed at early times which seems to correspond to this brief appearance of high-energy electrons. By the time the microwaves are switched off all three quantities have reached steady-state values. After the microwaves are switched off, n and T_e decay, due mainly to obstacle losses and excitation losses respectively, while T_i rises at first due to the improved electron-ion coupling at lower electron temperatures.

B. Averaging Probe

Since SIMULT deals only with average quantities, a Langmuir probe was constructed to give spatially averaged measurements. Its shape is that of a cylinder of revolution, extending across the plasma "bridge" region between one ring and the wall. Its radius varies with distance along its axis in such a way that each cylindrical element of surface area is proportional to the volume of space connected to that element by lines of magnetic flux. That is, the radius r as a function of distance x along the axis is a solution of the differential equation $2\pi r \sqrt{1 + \left(\frac{dr}{dx}\right)^2} \propto \frac{dV}{d\psi} \frac{d\psi}{dx}$. ψ is the usual poloidal flux function: $\psi(R, z) = \int_0^R 2\pi \rho B_z(\rho, z) d\rho$

where R is the radius from the major axis in cylindrical co-ordinates. $\frac{dV}{d\psi} d\psi$ is the volume of space between flux surfaces corresponding to ψ and $\psi + d\psi$, and $\frac{d\psi}{dx}$ is the derivative of ψ along the axis of the probe. The probe is shown in position in Fig. (1).

In the experiment discussed here the probe was simply biased at -45 V to collect ion saturation current. If the properties of the plasma are constant along a line of magnetic flux, and the same for all lines labeled by the same value of ψ including those which only encircle a single ring, then this measurement gives a true spatially averaged value for ion saturation current. This probe can also be used as an admittance probe¹². If in addition to the previous assumptions the temperature gradients in the plasma are not too large then the admittance measurement yields good approximations to the spatially averaged values of density and electron temperatures. This has been verified by measuring point-by-point profiles along the location of the averaging probe and calculating the appropriate weighted averages.

C. Comparison of Time Dependence

In this experiment only ion saturation current was measured; in the units used in the program, for j_{oi} in mA/cm²,

$$j_{oi} = 0.104 n \sqrt{\max(T_e, T_i)}. \text{ Fig. (3) shows the comparison between}$$

prediction and experimental measurement of ion saturation current for the same parameters as in Fig. (2). The steady-state values agree quite well in the supported case. In the levitated case there is a large discrepancy; in fact, the computer prediction does not even reach a steady state. This indicates the presence of some loss mechanism not accounted for in the computer prediction, only a little less important than losses to the hoop supports. In both cases the plasma buildup occurs somewhat later in the experiment than in the prediction: this could be due to some loss mechanism not properly treated in the program, or a 30% error in measuring the quantity of neutral gas admitted to the machine would have the same effect. The prediction and measurement of plasma decay after the microwaves are turned off look quite different. This may be due to the motion of the plasma as field lines leave the machine in the falling half of the pulse, a phenomenon which depends on the details of the magnetic field configuration and spatial distribution of the plasma, and is taken into account only crudely in the program.

D. Comparison of Scaling

One of the main uses of a zero-dimensional simulation program such as this might be to predict scaling laws for magnetic confinement devices. Accordingly, comparisons between prediction and experiment were made of the peak value attained by the ion saturation

current at the time the microwaves were turned off, while experimental parameters were varied. In most cases this peak value was a steady-state value.

Such a comparison is shown in Fig. (4), which gives the peak value of ion saturation current for varying microwave powers from .7 to 25 watts. At higher powers the scaling with microwave power is quite similar for prediction and experiment, though as in Fig. (3) the difference between levitated and supported cases is somewhat less than predicted. Both experiment and prediction show a knee around 1.5 watts; this is due to the fact that below this power the plasma buildup occurs so late that it is still going on at 22 msec. Thus the low-power end of the curve does not represent steady-state values but depends on the details of the plasma buildup.

Fig. (5) shows the comparison of peak values of ion saturation current for varying neutral gas pressures from 10^{-6} to 10^{-4} torr. The scaling of prediction and experiment agree quite well; a 50% error in measuring the neutral pressure would bring them into good quantitative agreement. The sharp knee in this example is similarly due to the fact that at low neutral pressures the plasma buildup occurs so late that it is still going on, or has hardly started, at 22 msec.

V. CONCLUSIONS

This simulation program, despite its admitted crudeness, provides surprisingly good agreement with experimental measurements. The discrepancies may provide information about anomalous loss processes; the agreements may provide information about scaling in toroidal magnetic confinement devices.

VI. ACKNOWLEDGMENTS

It is a pleasure to acknowledge the help of J. R. Patau in the development of the computer program and for the refinement of several of the terms in the differential equations. We are also grateful to Paul Nonn for doing the tricky job of machining the averaging probe.

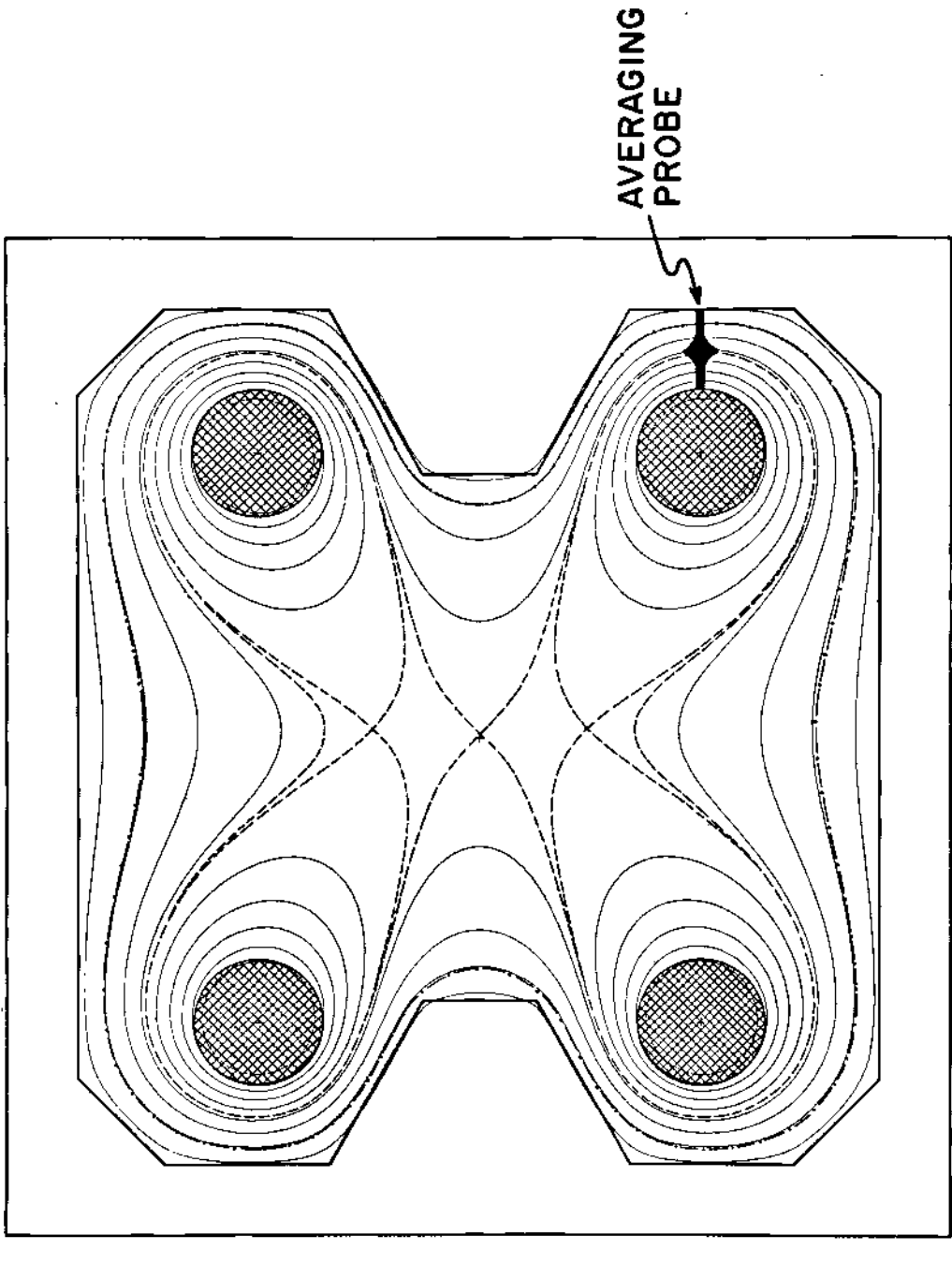
REFERENCES

1. J. R. Patau and J. C. Sprott, *Bull. Am. Phys. Soc.* 18, 1352 (1973).
2. H. K. Forsen, D. W. Kerst, R. A. Breun, A. J. Cavallo, J. R. Drake, and J. C. Sprott, Proceedings of the Fourth International Conference on Controlled Fusion and Plasma Physics, Rome (1970) p. 24.
3. J. F. Etzweiler and J. C. Sprott, *Bull. Am. Phys. Soc.* 18 1298 (1973).
4. H. W. Drawin, Collision and Transport Cross Sections, Report EUR-CEA-383, Association-Euratom-CEA, Fontenay-Aux-Roses (Seine) France (1967).
5. L. Kovrizhnykh, *Zh Eksp. Teor. Fiz.* 56, 877 (1969) [*Sov. Phys. - JETP* 29, 475 (1969)].
6. J. C. Sprott, Univ. of Wisconsin, Ph.D. Thesis (1969).
7. L. Spitzer, Jr., Physics of Fully Ionized Gases, Wiley Interscience, New York (1962).
8. D. J. Rose and M. Clark, Jr., Plasmas and Controlled Fusion, MIT Press, Cambridge (1961).
9. R. H. Loveberg in Plasma Diagnostic Techniques, R. H. Huddlestone and S. L. Leonard, eds., Academic Press, New York (1965), p. 98.

10. D. W. Koopman, Phys. Rev. 154, 79 (1967); J. B. H. Stedeford and J. B. Hasted, Proc. Roy. Soc. (London) A227, 466 (1955); P. M. Stier and C. F. Barnett, Phys. Rev. 103, 896 (1956).
11. J. H. Simons, et. al., J. Chem. Phys. 11, 307 (1943); W. H. Cramer, J. Chem. Phys. 35, 836 (1961).
12. J. C. Sprott, Rev. Sci. Inst. 39, 1569 (1968).

FIGURE CAPTIONS

- Fig. (1) Minor cross section of the Wisconsin Levitated Toroidal Octupole, showing lines of magnetic flux at 20 msec. after start of magnetic field pulse. Also shown is position of averaging probe. (Probe not to scale).
- Fig. (2) Computer prediction of n , T_e , and T_i time histories. $B_0 = 1$ kG, $p_{oi} = .125 \times 10^{-5}$ torr, $P = 25$ W, hoops supported. (Semilog plot).
- Fig. (3) Comparison of computer prediction (solid lines) and experimental measurement (dots) of ion saturation current time histories. Same parameters as for Fig. (2), hoops supported and levitated.
- Fig. (4) Comparison of computer prediction (solid lines) and experimental measurement (dots) of peak ion saturation current for varying microwave power. Other parameters are the same as for Fig. (2), hoops supported and levitated. (Log-log plot).
- Fig. (5) Comparison of computer prediction (solid line) and experimental measurement (dots) of peak ion saturation current for varying neutral pressure. Other parameters are the same as for Fig. (2). (Log-log plot).



TIME = .020 SEC

FIGURE 1

← TO AXIS

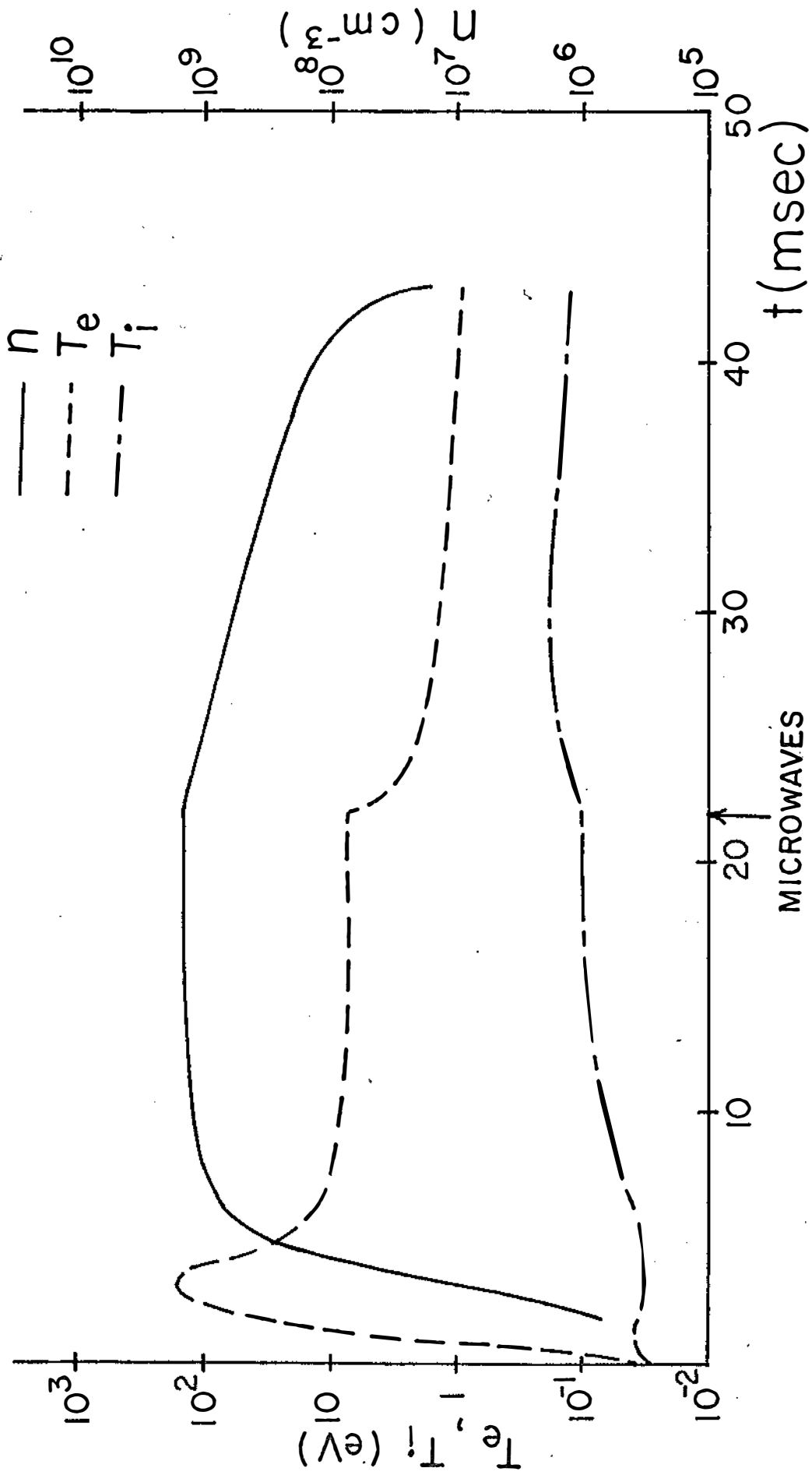


FIGURE 2

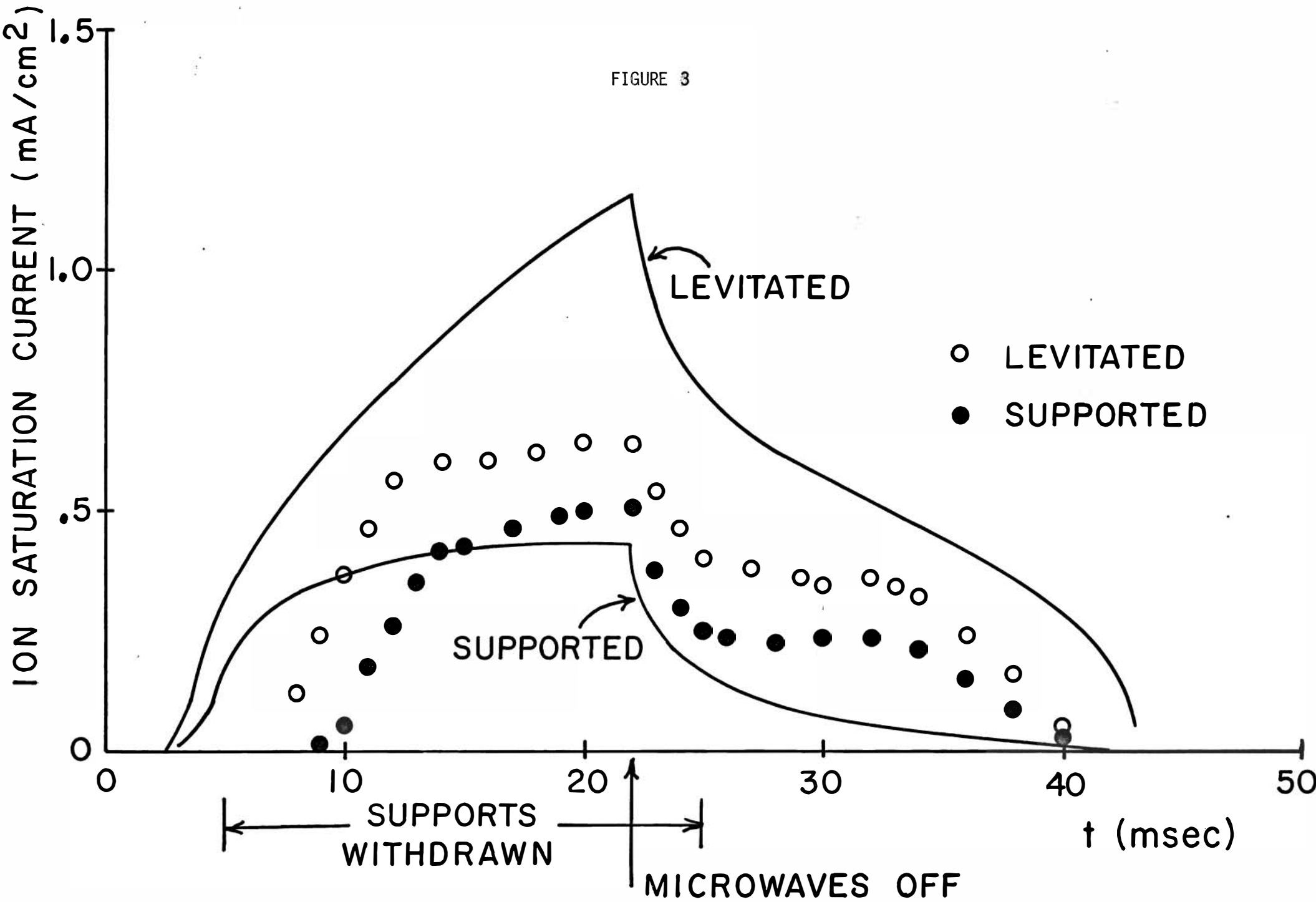


FIGURE 4

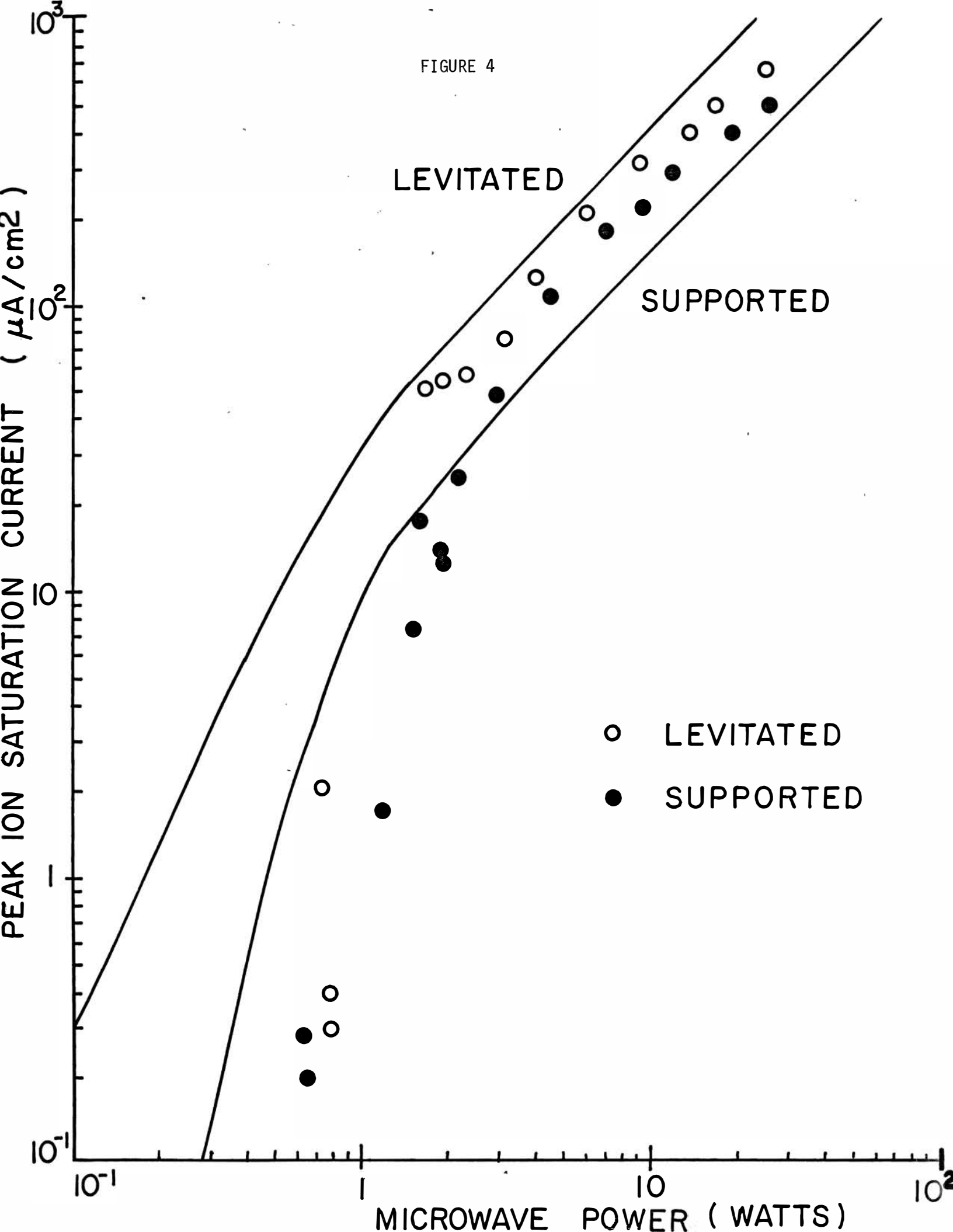


FIGURE 5

